Nat Hazards (2007) 42:361–378
DOI 10.1007/s11069-006-9086-x

ORIGINAL PAPER

Variation of coastal atmospheric boundary layer characteristics with convective activity along the west coast of India during the Arabian Sea Monsoon Experiment (ARMEX) 2002

N. V. Sam · U. C. Mohanty · A. Routray · S. Basu

Received: 19 July 2005 / Accepted: 24 September 2006 / Published online: 3 May 2007

Abstract This paper investigates the characteristic features of the coastal atmospheric boundary layer (CABL) along the west coast of India during the south-west monsoon (SWM) 2002. Extensive surface and upper-air findings were obtained during the same period from the Arabian Sea Monsoon Experiment (ARMEX; 15th June to 15th August 2002) 2002. The operational general circulation model (GCM) of the National Centre for Medium Range Weather Forecasting (NCMRWF) was used in this study to see the spatial variation of the CABL during two specific convective episodes that led to heavy rainfall along the west coast of India. The impact of a non-local closure (NLC) scheme employed in the NCMRWF GCM was carried out in simulating the CABL. The same episodes were also simulated using a similar parameterization scheme employed in the high resolution mesoscale modelling system (MM5). The diurnal variation of CABL is better represented from MM5 simulation. Comparing the MM5 simulation with that of the coarser grid NCMRWF GCM, we observed that the NCMRWF GCM underestimates the values of both latent heat flux (LHF) and the coastal atmospheric boundary layer height (CABLH). Results from MM5 therefore indicate that the best way to move forward in addressing the short-comings of coarse grid-scale GCMs is to provide a parameterization of the diurnal effects associated with convection processes.

Keywords Boundary layer · South west monsoon · ARMEX · Heavy rainfall · Latent heat flux

N. V. Sam · U. C. Mohanty (✉) · A. Routray
Centre for Atmospheric Sciences, Indian Institute of Technology, Hauz Khas, New Delhi 110016, India
e-mail: mohanty@cas.iitd.ernet.in

S. Basu
National Centre for Medium Range Weather Forecasting, Noida, UP, India

1 Introduction

Most of the rainfall over the Indian peninsula during the south-west monsoon (SWM) occurs in association with convective activity over the Arabian Sea (AS) and the Bay of Bengal (BOB) that propagates into the peninsula. These rainfall activities are usually associated with mesoscale convective systems embedded in a large-scale synoptic system over the AS. Several investigators have also studied the interaction of the low-level jet with Western Ghats that leads to substantial rainfall during the SWM. The analysis by Krishnamurti et al. (1983) shows that maximum rainfall rate along the west coast of India could be as high as approximately 20 cm a day.

Observations also indicate (Asnani 1993) that during the SWM there is a significant inflow of moisture from the southern regime between 0° N and 30° N. The latent heat of water vapour that is set free in the moist south-west current over land leads to the enhancement of convective currents and cloud growth (Basu et al. 1999), which, to a great extent, depends on the characteristics of the planetary boundary layer (PBL). Therefore, it is very important for one to understand the processes that characterize the PBL in the development and sustenance of semi-permanent features such as heat low, off-shore trough, monsoon low-level jet (MLLJ), and other low-level processes that bring in copious amount of rainfall during the SWM.

While there is a good understanding of homogeneous marine and land boundary layers, their variation is complicated when seen through the inherent heterogeneity observed in the coastal atmospheric boundary layer (CABL). Most coastal environments are modified by the adjacent ocean, the coastal topography and the land–sea thermal contrasts. Complex feedbacks occur between the atmosphere, ocean and land. The thermal contrast between the land and sea creates the land–sea breeze, coastal atmospheric fronts, and coastal ocean currents and upwelling. The convergence of marine air over the coastline can result in strong convection with heavy precipitation and runoff (Rogers 1995). Recent research has focused on thermally driven circulation, orographically forced events and land-falling storms due to mesoscale and large-scale interactions. But these processes are not mutually exclusive, and most environments are often affected by more than one of these systems (Wilczak et al. 1991).

One of the prime objectives of this study was to see the spatial distribution of CABL characteristics in promoting active convection leading to heavy rainfall along the west coast of India during the SWM of 2002. During the same period (SWM 2002) a major observational field campaign, the Arabian Sea Monsoon Experiment (ARMEX), was carried out by the Department of Science and Technology (DST), India, that provided, for the first time, extensive surface and upper air findings along the west coast of India. Details of this experiment can be found on the National Centre for Medium Range Weather Forecasting (NCMRWF) website (http://www.ncmrwf.gov.in). Most of the previous experimental campaigns have made observations over the Indian Ocean, BOB and AS, but none of these experiments could make intense observations along the Indian west coast or, especially, in the exclusive economic zone (EEZ). Thus, the observations from ARMEX-I have facilitated the study of the inherently heterogeneous CABL, wherein interactions between sea breezes, mesoscale eddies and terrain-generated winds can cause complex flow patterns (Wilczak et al. 1991; Douglas and Kessler 1991; Ulrickson 1992).

Some of the questions that are addressed in this paper are: the variations encountered in the structure of the CABL along the west coast during active convection; the spatial distribution of coastal atmospheric boundary layer height (CABLH), and the surface fluxes associated with imitating and maintaining the convective activity that are simulated when the NCMRWF general circulation model (GCM) and mesoscale modelling system (MM5) are used. As a result, this paper envisages the nature and role of convective systems in modulating the CABL along the west coastal zone of the Indian peninsula during the SWM.

2 Data and initial conditions

2.1 NCMRWF GCM

The NCMRWF GCM is an adapted version of the National Centre for Environmental Prediction (NCEP), 18-layer spectral model having a terrain-following coordinate system. Relative vorticity, divergence, virtual temperature, surface pressure and specific humidity are the main prognostic variables in the model. Monin–Obukov similarity theory and bulk aerodynamic formulations are used in the surface layer, while the eddy transport that takes place through the mixed layer is dependent on the Richardson number, which stands as a criterion for the vertical diffusion processes. The details of the NCEP forecast and assimilation model system are given in Kanamitsu (1989) and Parish and Derber (1992). The overview of the NCMRWF model is given in Table 1.

The NCMRWF GCM has the option for using three different PBL parameterization schemes namely (a) First-order local closure or *K*-theory; (b) non-local closure [NLC, Hong and Pan 1996 (HP)], and (c) the TKE-ε scheme. All of these three schemes have been tested separately to examine their performances in simulating boundary layer characteristics during different convective episodes over the Indian seas (Sam 2005), of which it has been clearly found that NLC-HP fared better among the three. Therefore, the present study was undertaken using NLC-HP. A detailed description of the scheme (NLC-HP) is also given by Basu et al. (1999, 2002) and Sam (2005).

2.1.1 Initial conditions for NCMRWF GCM

The NCMRWF GCM was run during ARMEX-I(2002), and two specific periods of convective activities over the Arabian Sea off the west coast of India were selected for the study of the spatial variation of MBL characteristics. The analysis fields valid for 0000 Coordinated Universal Time (UTC) of the 19th June and 3rd August 2002 were used as initial conditions for the global model. These two cases will be referred to as case 1 and case 2, respectively. The model was then integrated for 5 days to obtain the forecasts. The output of the model forecast due to NLC-HP was stored for comparison.

Figures 1 and 2 show the NCMRWF GCM wind analysis (925, 850, 700, 500 and 150 hPa levels) and the precipitable water content at 0000 UTC on 20th June and 4th August 2004, respectively. The off-shore trough running from the south Gujarat coast off the Kerala coast persists on 20th June 2002 (Mohanty et al. 2002). A shear line at 7.5 km, extending from the AS to the BOB, close to 15° N, is observed during

Table 1 Brief description of the NCMRWF GCM (T-80)

Model elements	Components	Schemes
Grid	Horizontal	T-80, spectral, global
	Vertical	18 sigma layers [σ = 0.995, 0.981, 0.960, 0.920, 0.856, 0.777, 0.668, 0.594, 0.497, 0.425, 0.375, 0.325, 0.275, 0.225, 0.175, 0.124, 0.74, 0.21]
Dynamics	Prognostic variables	Rel. vorticity, divergence, virtual temp., log surface press, water vapour mixing ratio
	Horizontal transform	Orzag's technique
	Vertical differencing	Arakawa's energy conserving scheme
	Time differencing	Semi-implicit (divergence, surface press and virtual temp.)
		Explicit leap-frog (vorticity and mixing ratio)
	Time filtering	Robert's method
	Horizontal diffusion	Fourth order
Physics	Surface fluxes	Monin and Obukhov similarity
	Turbulent diffusion	*K*-theory
	Radiation	Short wave—Lacis and Hansen (1974)
		Long wave—Fels and Schwarzkopf (1975)
	Deep convection	Kuo scheme modified
	Shallow convection	Tiedtke method (Tiedke 1983)
	Large-scale condensation	Manabe-modified
	Cloud generation	Slingo scheme (Slingo 1987)
	Rainfall evaporation	Kesslers's scheme
	Land surface processes	Pan method
	Gravity wave drag	Lindzen (1981)

this period (case 1). On 4th August 2002 (Fig. 2), a trough on the sea level lies off the Karnataka and Konkan–Goa coast. Cross-equatorial flow is observed into Arabian Sea between 40° E and 70° E at 925 hPa and 850 hPa. The general flow in the Arabian Sea is from the southwest direction, and the speed varies between

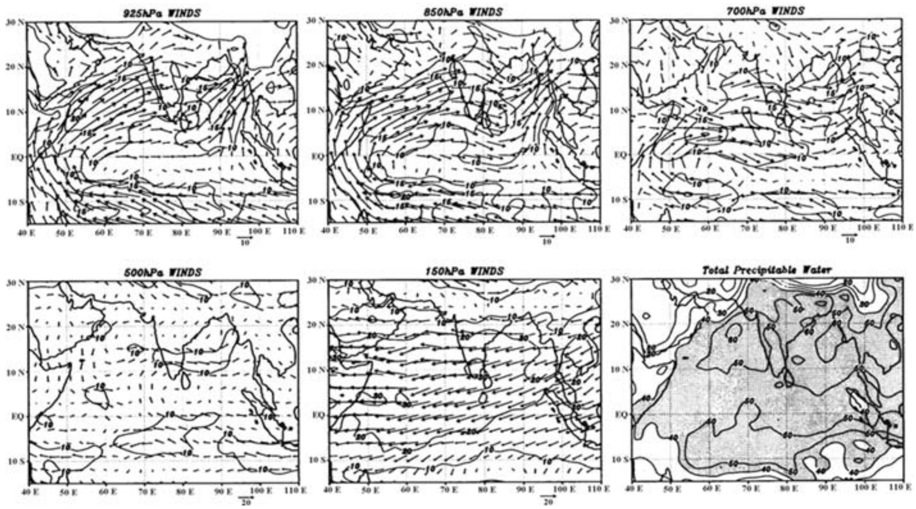

Fig. 1 NCMRWF GCM wind analysis on 20th June 2002 at 0000 UTC of the day at 925, 850, 700, 500 and 150 hPa and total precipitable water content of the atmosphere. The isotachs are at 5 m s^{-1} intervals till 700 hPa and, later, at 10 m s^{-1}. The precipitable water is expressed in millimetres

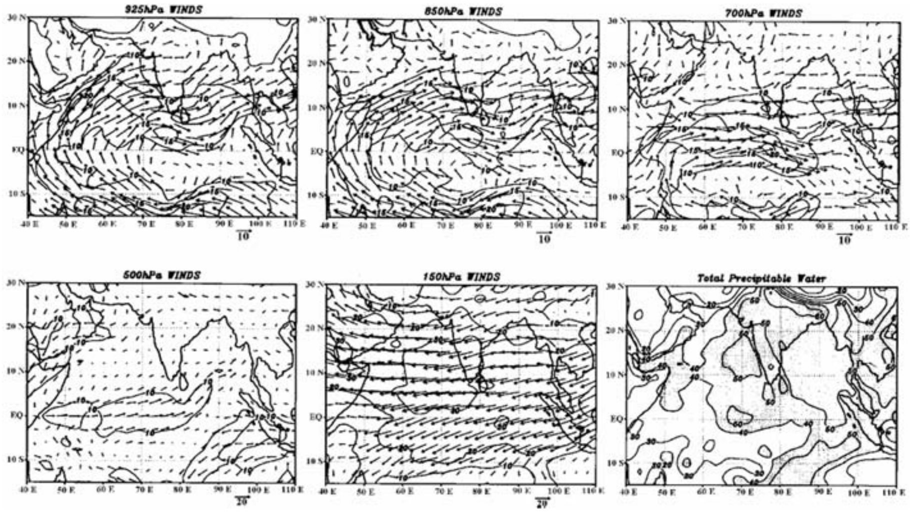

Fig. 2 Same as Fig. 1, but for 4th August 2002

10 m s^{-1} and 20 m s^{-1}. A cyclonic circulation at 400 hPa lies off the Konkan–Goa coast. The upper tropospheric easterlies at 150 hPa vary between 20 m s^{-1} and 30 m s^{-1}. The total precipitable water content (Fig. 2) in the western Arabian Sea varies between 30 mm and 40 mm, while, in the eastern Arabian Sea, it varies between 40 mm and 50 mm. Figure 3 shows the convective cloud bands over the Goa during case 1 (Fig. 3a) and case 2 (Fig. 3b).

2.2 Mesoscale modelling system version 3.6

The MM5 model (version 3.6) is a fifth-generation Pennsylvania State University/ National Center for Atmospheric Research (PSU/NCAR) limited-area mesoscale model, non-hydrostatic, terrain-following sigma co-ordinate, designed to simulate

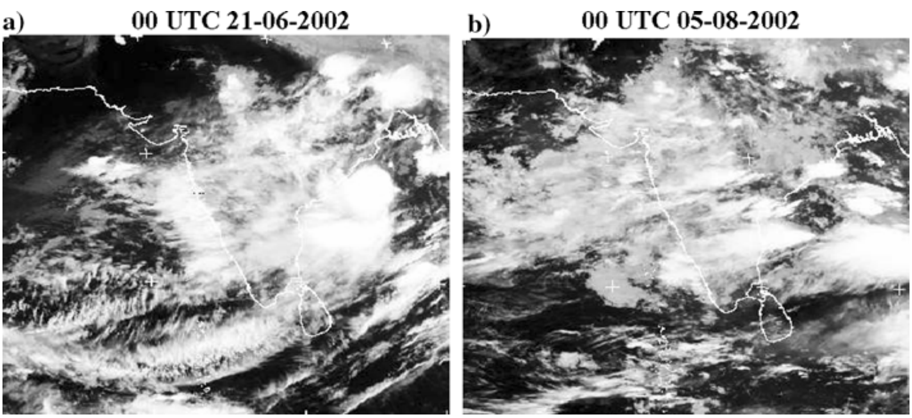

Fig. 3 Meteosat IR pictures locating Goa (one of the west-coast land stations) during the two different convective events **a** Case 1, **b** case 2

mesoscale and regional-scale atmospheric circulation (Dudhia et al. 2002). A logical combination of multiple-nest-domain configuration, variety of physical parameterization schemes and four-dimensional data assimilation technique makes the model capable of simulating a meteorological event on any scale. In this study MM5 is run using the Grell scheme (Grell et al. 1994) for cumulus parameterization and an NLC-HP scheme, also called MRF-PBL, for the boundary layer parameterization. The MM5 model configuration used in the present study is given in Table 2.

2.2.1 Initial conditions for MM5

The initial condition and lateral boundary conditions are obtained from NCEP global analysis. The initial condition has been improved with the insertion of additional observations through objective analysis. It is also used as a tool to interpolate and smooth the unwarranted spikes in the observed data. The meteorological data sets used in this study are categorized into regular and special observations (ARMEX-I). The heavy rainfall that has been observed during case 1 and case 2 could be, seemingly, the result of an off-shore trough that extended from Kerala to Maharashtra along the west coast of India. A cyclonic circulation (somewhat like a mid-tropospheric cyclone) has been noticed between 2.1 km and 7.6 km over the Saurashtra, Kutch and its neighbourhood (Mohanty et al. 2002).

The initial first-guess fields are taken from low-resolution (1° × 1°) global AVN (USA Aviations) analysis, except sea surface temperature (SST), which is extracted from the FNL (final analysis) global analysis. The special findings obtained during this period that are used to refine the first guess are as follows: (a) surface and

Table 2 MM5 model configuration used in this study

Parameter	Configuration		
Model	Fifth-generation (PSU/NCAR) MM5, version 3.6		
Dynamics	Non-hydrostatic with 3-D coriolis force		
Main prognostic variables	u, v, w, T, p′ and q		
Map projection	Mercator conformal mapping		
Central point of domain	Latitude 13.8° N, longitude 80.3° E		
Number of horizontal grid points	Coordinate	D-1 (15 km)	D-2 (5 km)
	Y	190	331
	X	185	223
Number of vertical levels	23		
Horizontal grid scheme	Arakawa B grid		
Time integration scheme	Leap-frog scheme with time-splitting technique		
Lateral boundary conditions	Nudging toward the NCEP/NCAR re-analysis		
Radiation scheme	Dhudhia's short-wave/long-wave simple cloud radiation scheme with frequency of 30 min		
PBL parameterization schemes	MRF-PBL		
Cumulus parameterization schemes	Grell		
Microphysics	Explicit scheme of Reisner (mixed phase)		
Soil model	Multi layer soil model		
Topography	30s elevation data [United State Geological Survey (USGS)]		
Sea surface temperature (SST) and surface parameters	SST (from Final Analysis (FNL) analysis); other surface parameters from AVN (NCEP analysis)		

upper-air data, both over the Arabian Sea off the west coast of India and west coast land stations; (b) satellite observations from QSCAT. The United State Geological Survey (USGS) 25-category global coverage data, having 15 min and 5 min resolution terrain, land use/vegetation, soil and land water mask, are used in the coarser and finer domain of the model, respectively. The model MM5 is run with double-nested domain (coarser domain 15 km and finer domain 5 km) from 19th June (1200 UTC) to 21st June (1200 UTC) 2002, i.e. for a period of 48 h, after 12 h analysis nudging from 19th June (0000 UTC) to 19th June (1200 UTC) 2002 during case 1. Similarly, during case 2, the model is run for 48 h from 3rd August (1200 UTC) after 12 h of analysis nudging. The double-nested MM5 model domain is given in Fig. 4.

3 Results and discussions

In this section the spatial distribution of CABL characteristics, viz., the variation in latent heat flux (LHF) and CABLH, as simulated by NCMRWF GCM and MM5, all through the two active convection periods that brought heavy precipitation during ARMEX-I (2002) are examined. This section also draws a comparison between NCMRWF GCM and MM5 simulations.

3.1 Spatial variation in LHF

The variation in LHF during these two specific episodes of convective activity (case 1 and case 2) during the 2002 Indian summer monsoon (ISM), when an off-shore trough persisted over the Arabian Sea off the west coast of India, simulated with the NLC-HP scheme (now operational at NCMRWF) is shown in Fig. 5a–d, e–h, respectively. In both of these cases during the 20th June and 4th August 2002, the

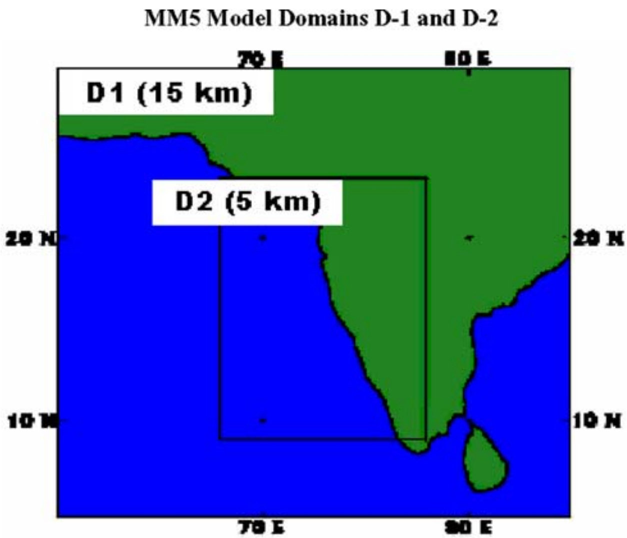

Fig. 4 MM5 model domains used in the present study

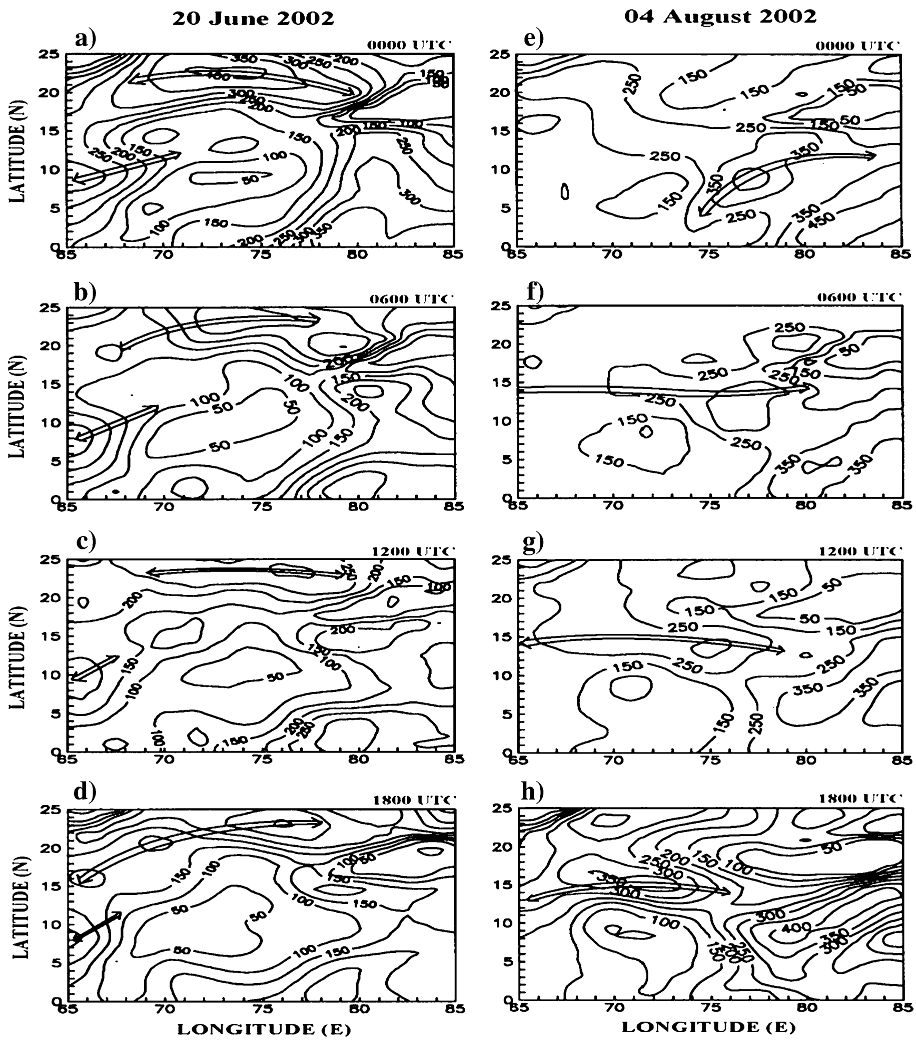

Fig. 5 Six hourly (0000, 0600, 1200 and 1800 UTC) NCMRWF GCM (T-80) simulated (2nd day forecast) spatial variation of LHF on 20th June 2002 (**a–d**) and 4th August 2002 (**e–h**) using the NLC-HP planetary boundary layer parameterization scheme

LHF values along the west coast were greater than 200 W m^{-2}. At Goa (13.38° E, 73.83° N) maximum precipitation of 620 mm was recorded on 21st June 2002. This observation very well corroborates with the distribution of the simulated LHF values shown in Fig. 5a–d. At 0000 UTC on 20th June 2002, LHF near Goa was around 200 W m^{-2}, while, during 0600, 1200 and 1800 UTC, it was ~150 W m^{-2}, 150 W m^{-2} and 100 W m^{-2}. During case 2, along the west coast, the LHF values on 4th August 2002 ranged between 200 W m^{-2} and 350 W m^{-2} (Fig. 5e–h). It can be observed from the synoptic conditions (Mohanty et al. 2002) that the convective conditions prevailed for a longer time (3–10 August 2002), marking the revival of monsoon activity. Higher values of LHF between 10° N and 20° N (marked by curved lines in Fig. 5a–d) shows the proximity of the ISM limit.

Also, similar lines are marked over high values of LHF on 4th August 2002 (Fig. 5e, f), depicting the strengthening of the monsoon current after the prolonged break-like condition observed during July 2002. The variations in LHF, as simulated by MM5 during case 1 and case 2, is given in Fig. 6(A) and (B), respectively. The diurnal variation is much pronounced in MM5 simulations depicted in both Fig. 6(A) (15 km; D-1 and 5 km; D-2) and (B) (15 km; D-1 and 5 km; D-2). The distribution of LHF due to MM5 is more or less similar, yet clearer, than that due to NCMRWF GCM. The diurnal variation in LHF is quite remarkable, with a demarcating difference in its evolution and distribution over land and marine atmosphere. The MM5-simulated LHF values are on the higher side and, on average, are higher by ~150–250 W m^{-2} in both of these cases and closer to the estimations (Sam et al. 2005). It is interesting to note that the D-2 (Fig. 6A, e–h; 5 km resolution) distribution of LHF is better than that of D-1 (Fig. 6A, a–d; 15 km resolution).

3.2 Coastal atmospheric boundary layer height

To predict any synoptic situation over the ocean, it is very important for one to understand the air–sea interaction processes that couple the ocean and atmosphere. The distribution of SST, and the magnitude of the wind stress forcing (Neelin 1990; Meehl 1990), are both intimately connected with the structure of the MBL. In the previous section the variation in LHF during such a prominent synoptic situation, viz., off-shore trough regime and associated convective processes, has been discussed. In this section the distribution of BLH over the same situations is elucidated. The boundary layer height in both the models is estimated from potential temperature profiles.

Coastal atmospheric boundary layer height simulated by NCMRWF GCM during case 1 (Fig. 7a–d) and case 2 (Fig. 7e–h) over the Arabian Sea off the west coast of India, when an off-shore trough is observed, ranged between 700 m and 1,100 m on both 20th June and 4th August 2002. The spatial and temporal growth of CABLH is well corroborated with the LHF values (Fig. 5) during these periods. During the ISM season, apart from comparatively warmer sea surface, the strong southwesterly monsoonal winds and low-level jet over the AS give rise to a fairly deep CABLH. The CABLH deepens as one approaches the coast line. This may be due to the orography of the Western Ghats.

Figure 8A and B show the variation in CABLH during case 1 and case 2 over the Arabian Sea along the west coast of India. During both the cases, the CABLH is noticed to be greater than 1,000 m, similar to that simulated by NCMRWF GCM (Fig. 7). However, a careful observation of the BLH elucidates a somewhat diurnal pattern of variation. Also, BLH values simulated by MM5 are higher (>200–500 m) than those simulated by the NCMRWF GCM and are closer to the estimated BLH over the Arabian Sea (onboard ORVSK) on 4th August 2002; it is 1,545 m at 0000 UTC and 1,461 m at 1200 UTC (Sam et al. 2005). The CABLH shows finer structure, which is not evident in the NCMRWF GCM model. The finer structure could be due to higher resolution of the model, representing convection in a better way.

3.3 Rainfall distribution along the west coast of India

Figure 9a and b show NCMRWF GCM forecasted (day 1) rainfall valid at 03Z 21st June 2002 and 03Z 5 August 2002, respectively. The observed 24 h accumulated

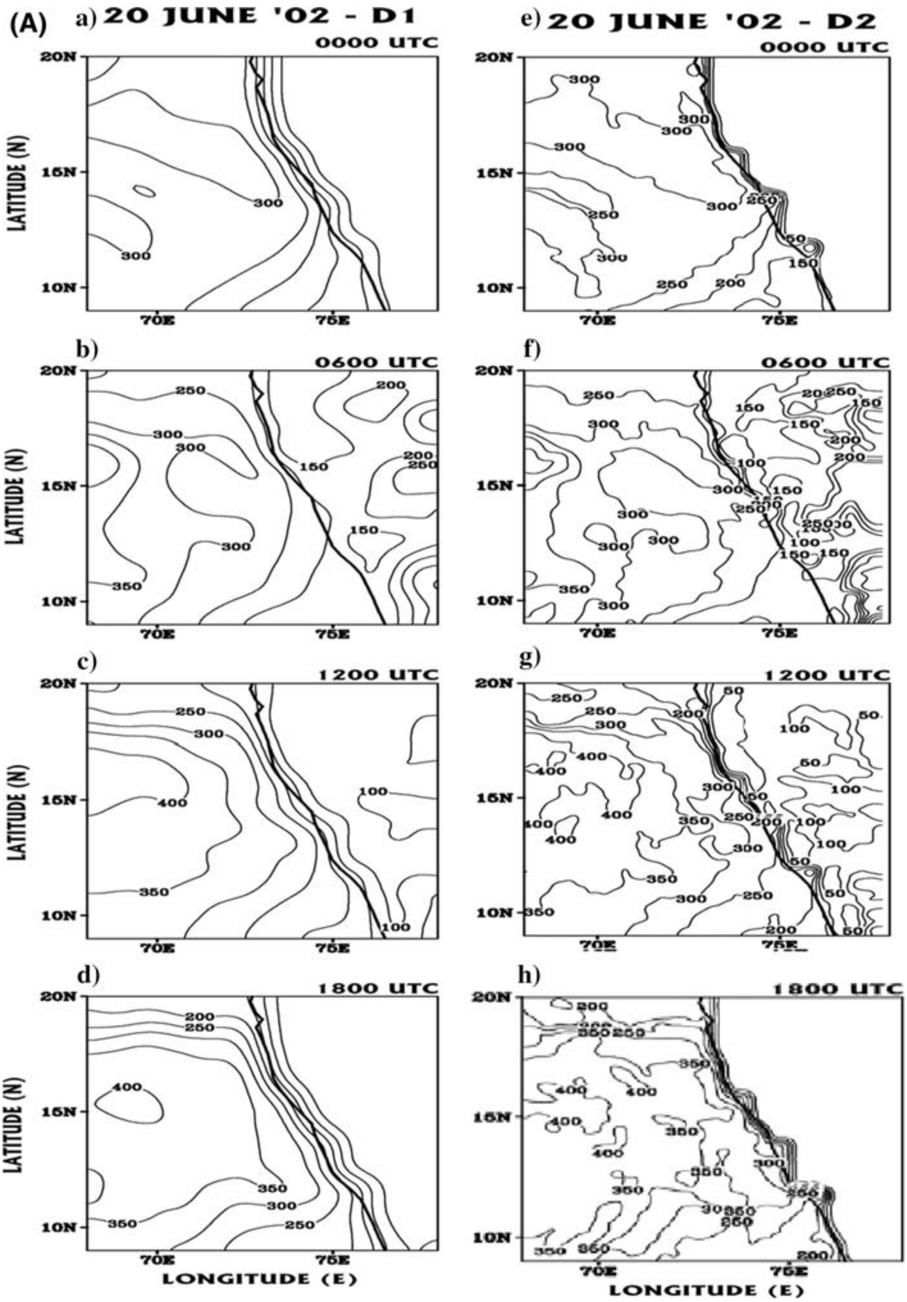

Fig. 6 **A** Six hourly (0000, 0600, 1200 and 1800 UTC) MM5-simulated spatial variation of LHF on 20th June 2002, where **a**–**d** represent domain D-1; 15 km, and **e**–**h** represent domain D-2; 5 km, using MRF (equivalent of NLC-HP) boundary layer parameterization scheme. **B** Six hourly (0000, 0600, 1200 and 1800 UTC) MM5-simulated spatial variation of LHF on 4th August 2002, where **a**–**d** represent domain D-1; 15 km, and (**e**–**h**) represent domain D-2; 5 km, using MRF (equivalent of NLC-HP) boundary layer parameterization scheme

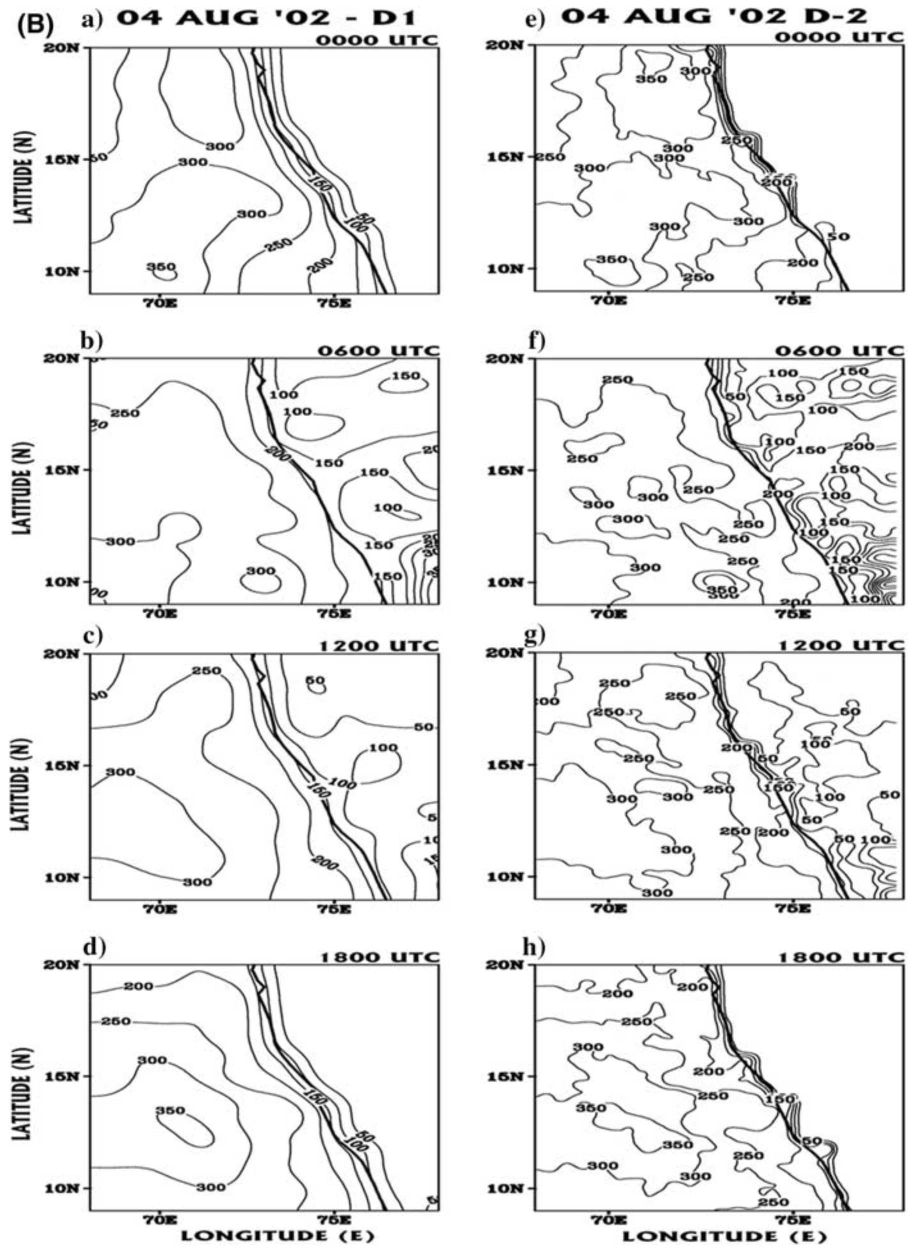

Fig. 6 continued

rainfall has been obtained from the Indian daily weather report (IDWR) for 0300 UTC on 21st June (Fig. 10a) and 5th August (Fig. 10d) 2002, respectively, along the west coast of India. Very heavy rainfall, amounting to 22 cm and 14 cm (during the last 24 h), respectively, is noticed over Ratnagiri in the Konkan and Goa regime on 21st June and over Mumbai on 5th August 2002. Comparing the

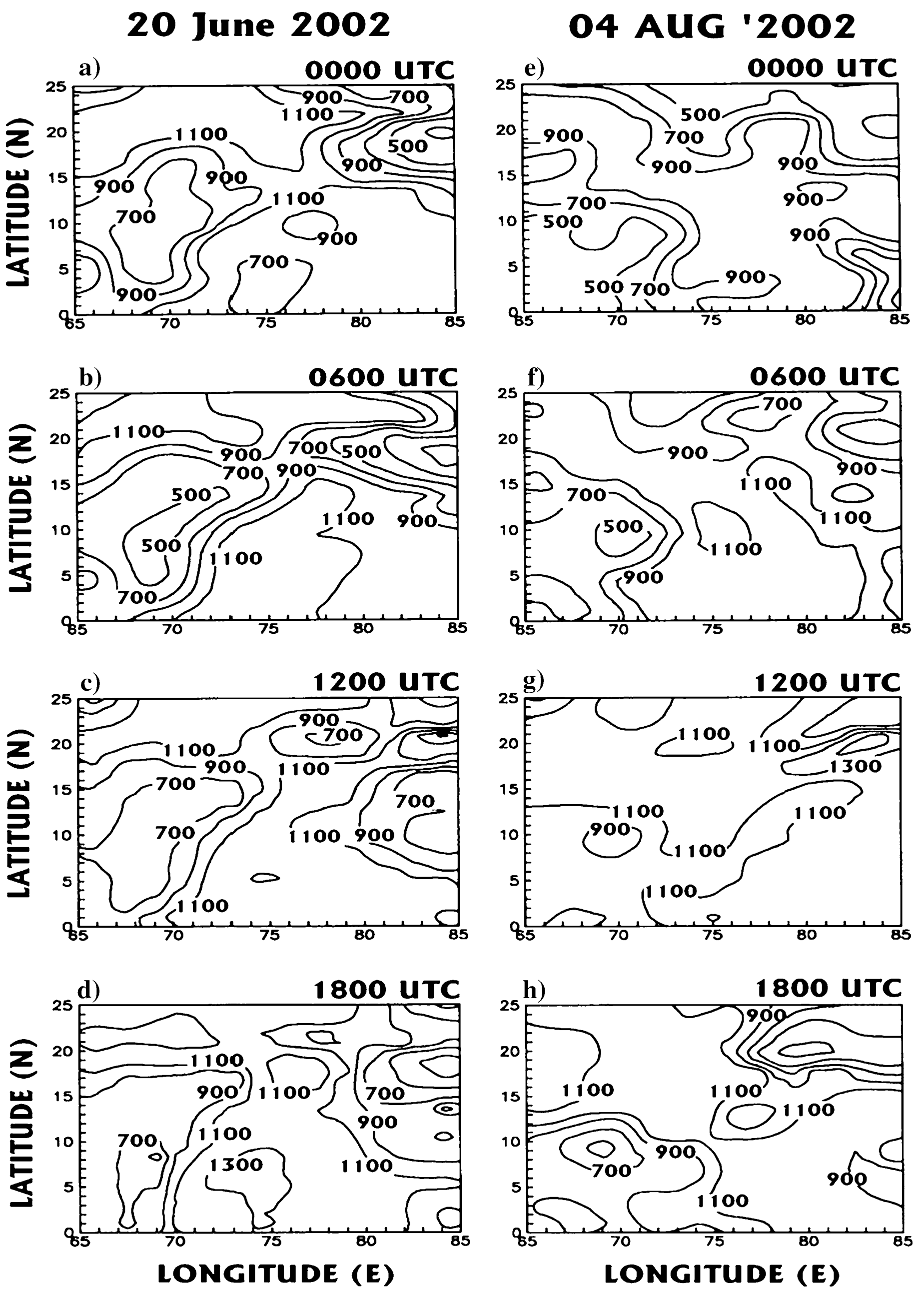

Fig. 7 Six hourly (0000, 0600, 1200 and 1800 UTC) simulated spatial variation of CABLH on 20th June and 4th August 2002 (NCMRWF GCM, T-80, 2nd-day forecast) over the Arabian Sea off the west coast of India during ARMEX (2002) using NLC-HP planetary boundary layer schemes. **a**–**d** represent the 20th June 2002 case, while **e**–**h** show the 4th August 2002 simulation

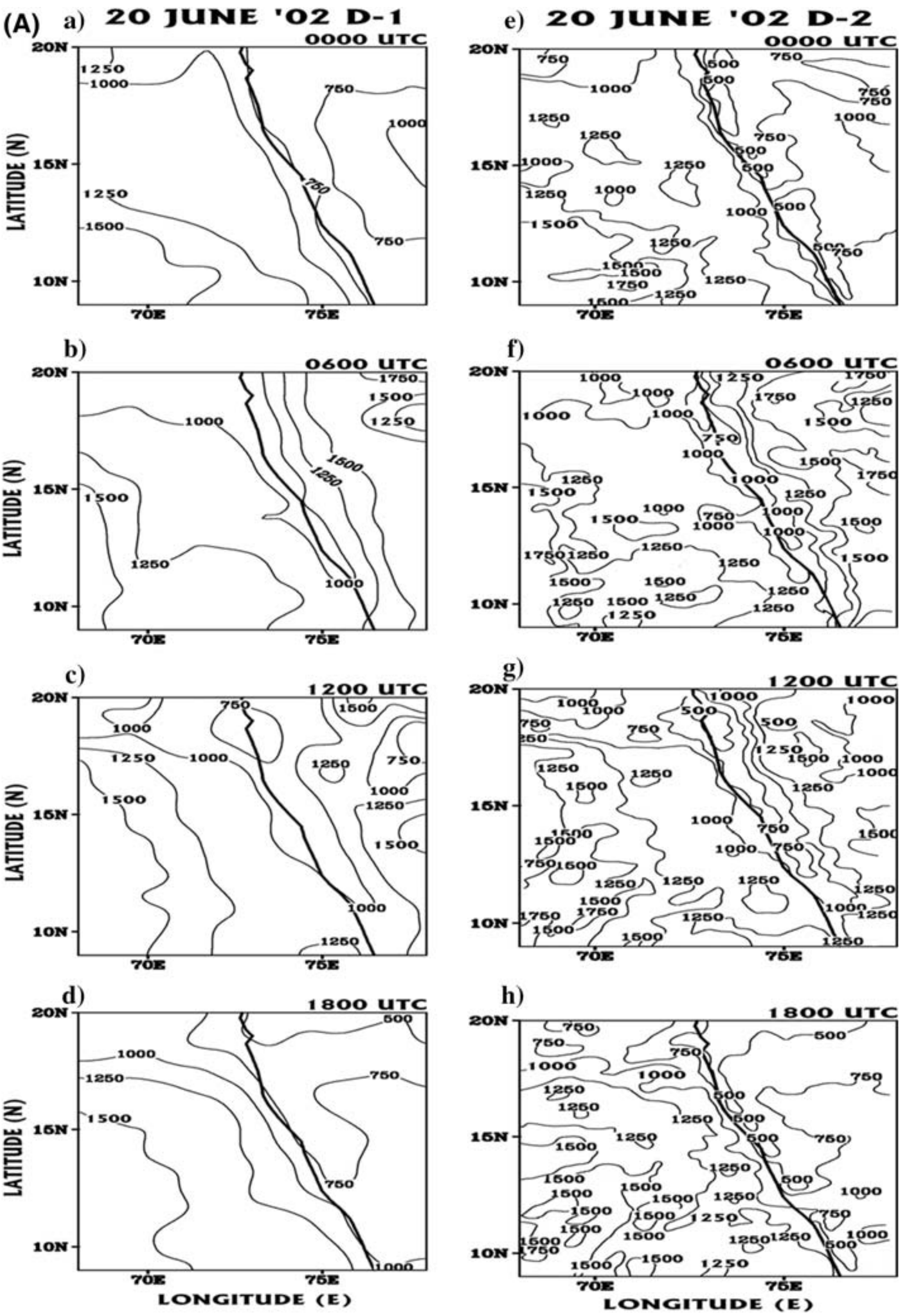

Fig. 8 **A** Six hourly (0000, 0600, 1200 and 1800 UTC) MM5-simulated spatial variation in CABLH on 20th June 2002, where **a–d** represent domain D-1; 15 km, and **e–h** represent domain D-2; 5 km, using MRF (equivalent of NLC-HP) planetary boundary layer parameterization scheme. **B** Six hourly (0000, 0600, 1200 and 1800 UTC) MM5-simulated spatial variation in coastal CABLH on 4th August 2002, where **a–d** represent domain D-1; 15 km, and **e–h** represent domain D-2; 5 km, using MRF (equivalent of NLC-HP) PBL parameterization scheme

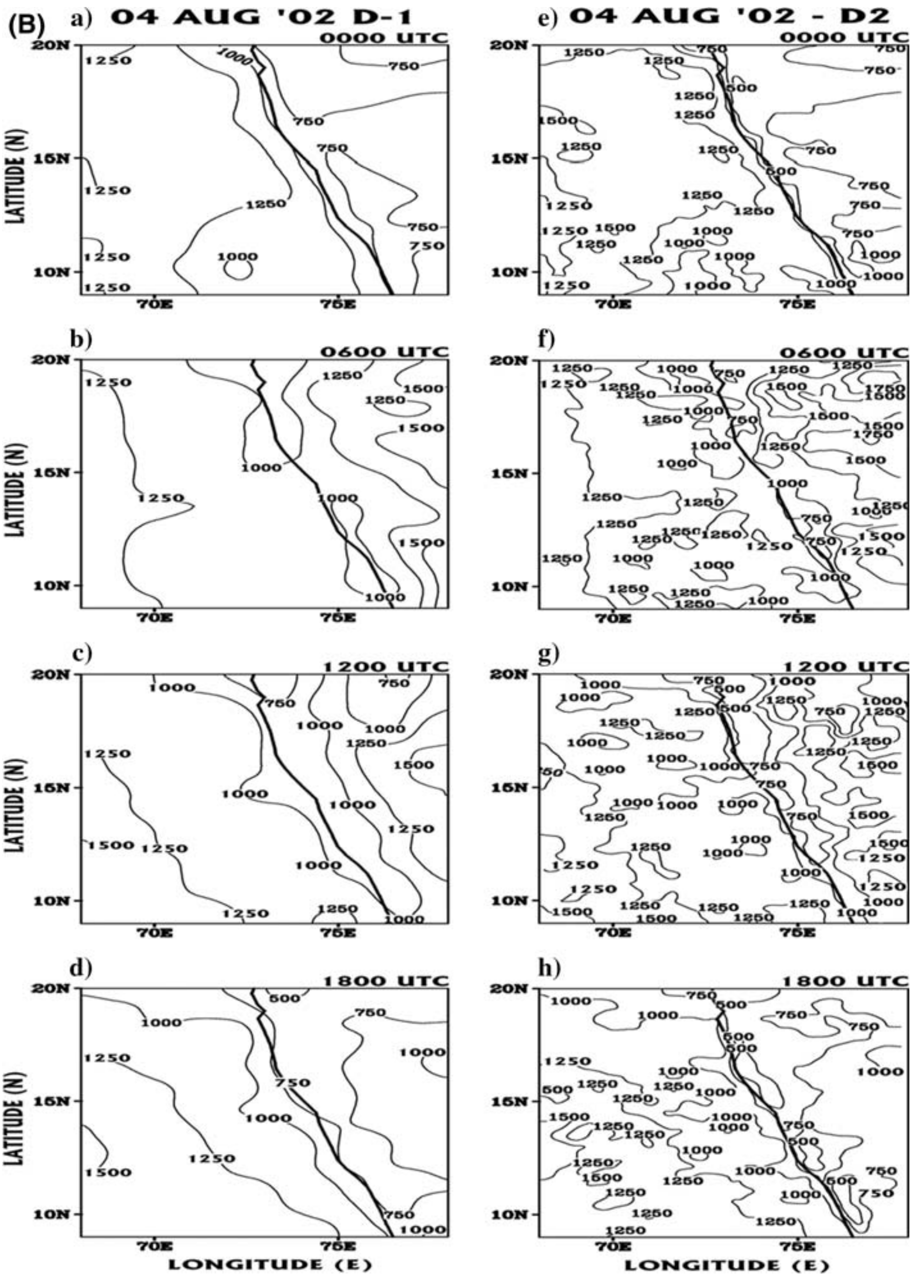

Fig. 8 continued

NCMRWF GCM day 1 simulated rainfall with the observed rainfall, one notices that the GCM values are under-predicted. The main reason for such an under-prediction of rainfall could be the coarser grid of NCMRWF GCM. A definite secondary reason could be the non-inclusion of additional observational data

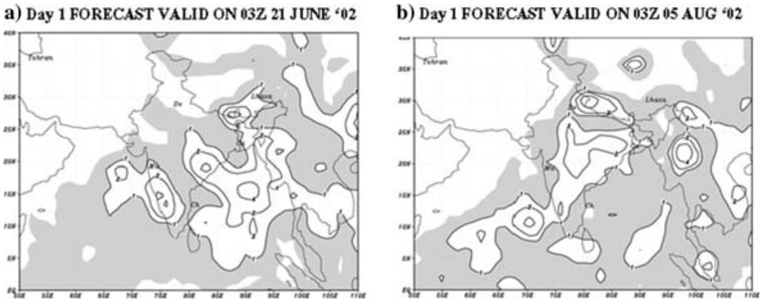

Fig. 9 NCMRWF GCM (T-80) predicted day-1 rainfall in centimetres (contour intervals = 0.1, 1, 2, 4, 8...), valid on (**a**) 03Z 21st June 2002 and (**b**) 03Z 5th August 2002

obtained during ARMEX in refining the initial analysis in the global analysis forecast system. Both of these shortfalls are more or less wiped out when one is simulating these heavy rainfall events (case 1 and case 2) using MM5, as it is run by refining the initial input by additional observations from ARMEX and by having a high-resolution (5 km and 15 km) configuration.

Figure 10b, c, e, f, respectively, depict the MM5-simulated 24 h accumulated rainfall along the west coast of India on 21st June and 5th August 2002. Figure 10b and e show domain 1 (D-1; 15 km resolution) simulated rainfall, while Fig. 10c and f show domain 2 (D-2; 5 km resolution). The MM5-simulated rainfall distributions (Fig. 10b, c, e, f) along the west coast of India show the clear presence of organized convective activity leading to this kind of precipitation. The effect of the off-shore trough observed over the Konkan–Goa regime, and the presence of mid-tropospheric circulation (MTC) over the Arabian Sea off the west coast of India, especially over the north Maharashtra and Gujarat coast, are the causative features of this heavy rainfall over these regions (Mohanty et al. 2002).

Looking at an overall picture of the simulated rainfall, one observes that the rainfall is still less than the observed one. However, in comparison with the NCMRWF GCM (coarser grid model) simulations, the MM5 experiments produced simulations closer to the observations (Fig. 10; Table 3). In fact, the localized distribution of rainfall during both 21st June and 5th August are better represented by the 5 km (Fig. 10c, f) resolution simulations than by the 15 km ones (Fig. 10b, e). The position of maximum rainfall (22 cm) on 21st June, recorded at Ratnagiri (16.6° N, 73.2° E), is well represented in all the simulations. This location is more accurately captured by the 5 km resolution (Fig. 10c; D-2) simulation. The second maximum rainfall (11 cm), observed over Mumbai, is also well represented in D-2 domains (Fig. 10c). Although the location of heavy rainfall is well simulated in the D-2 domains, the amount is on the lower side. This could be mainly attributed to the presence of orography (Western Ghats) that needs better representation in the model. Also, it awakens the possibility of a further refining of the convective parameterization schemes, together with their interaction with surface and boundary layer processes.

During case 2, the highest rainfall (14 cm) observed was over Mumbai, along the west coast. Synoptic and observational analyses suggest (Sam et al. 2005; Mohanty et al. 2002) that the MTC is a little weakened and is spread over a larger area. The rainfall distribution pattern (Fig. 10e, f), too, shows larger coverage over the Arabian Sea off the west coast of India. The overall distribution of the rainfall

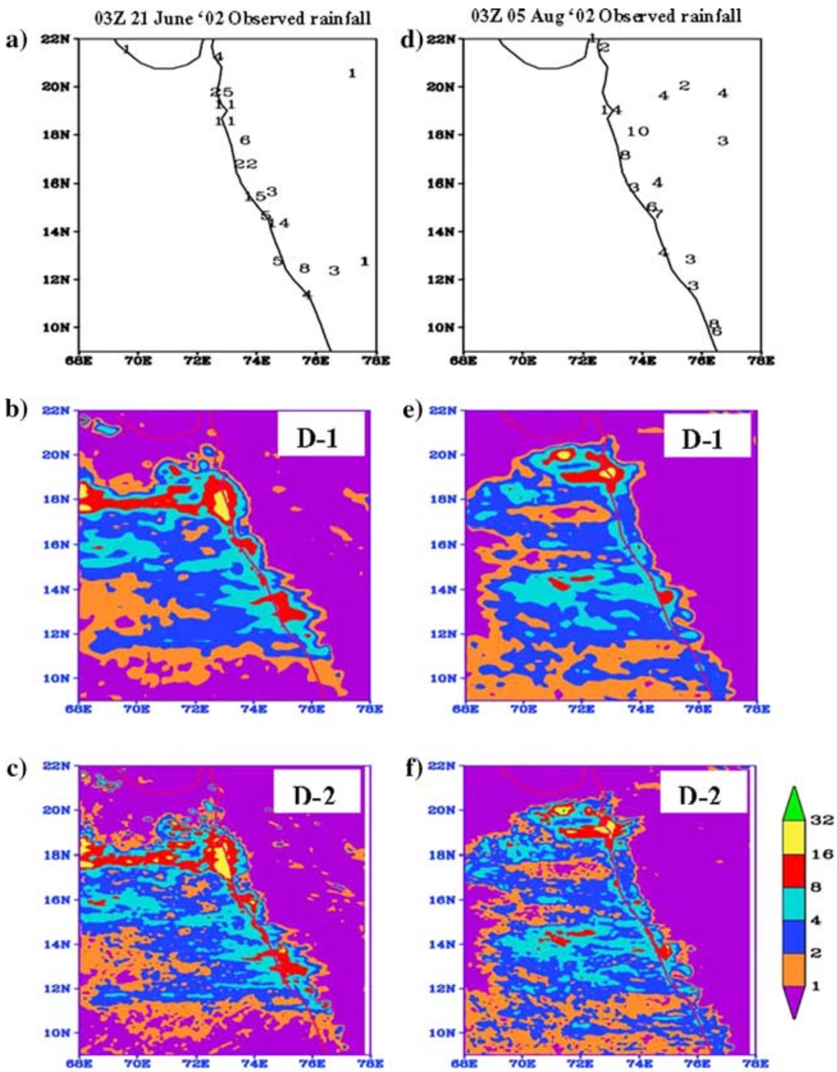

Fig. 10 Observed rainfall (cm) along the west-coast stations of India, valid for (**a**) 21st June and (**d**) 5th August 2002. **b** and **c** Show the MM5-simulated rainfall (cm) valid for 21st June 2002 over D-1 (15 km) and D-2 (5 km), respectively; similarly **e** and **f** show the MM5-simulated rainfall valid for 5th August 2002 over D-1 (15 km) and D-2 (5 km)

pattern due to both the 15 km (Fig. 10e) and 5 km (Fig. 10f) resolution (D-1 and D-2) experiments, represents reasonably well the observed synoptic condition along the west coast of India. In-depth analysis shows that D-2 simulations (during both case 1 and case 2) are able to capture the location and amount of rainfall better than D-1 simulations can. However, it needs to be mentioned here that MM5 is not able to represent adequately the rainfall pattern over the Saurashtra region of Gujarat, in D-1, while D-2 (Fig. 10c, f) simulation is able to show light/little rainfall over that region.

Table 3 Comparison between observation and model simulation by station

Station name	Latitude (deg)	Longitude (deg)	Observed rainfall (cm)	Model-simulated rainfall (cm)	
				D-1	D-2
(a) 24 h accumulated rainfall valid at 0300 UTC 21st June 2002					
Surat	21.1	72.5	4	2	3
Mahabaleswar	17.6	73.4	6	4.7	5.5
Mumbai	18.5	72.5	11	10	11.7
Panjim	15.3	73.5	15	4.5	5.8
Ratnagiri	16.6	73.2	22	8.8	10.2
Alibag	18.4	72.5	11	10	11.2
Belgaum	15.5	74.3	3	2.4	3.1
Honavar	14.2	74.3	14	8.2	9.1
Karwar	14.5	74.1	5	5.5	4.6
Mangalore	12.6	74.5	5	4.6	4.7
Medikeri	12.3	75.4	8	7.1	8.3
Kozhikode	11.2	75.5	4	3.3	3.9
(b) 24 h accumulated rainfall valid at 0300 UTC 5th August 2002					
Mahabaleswar	17.6	73.4	10	8.7	9.6
Mumbai	18.5	72.5	14	3.2	4.1
Panjim	15.3	73.5	3	2.5	3.1
Parbhani	19.2	76.5	4	1.5	2.0
Ratnagiri	16.6	73.2	8	6.9	7.8
Belgaum	15.5	74.3	4	3.4	3.7
Honavar	14.2	74.3	7	5.9	6.2
Karwar	14.5	74.1	6	4.8	5.7
Mangalore	12.6	74.5	4	3.9	4.2
Medikeri	12.3	75.4	3	2.1	2.5
Alapuzha	9.3	76.3	6	1.3	1.5
Cochi	9.6	76.2	8	2.4	3.5
Kozhikode	11.2	75.5	3	2.3	3.0

4 Summary and conclusions

The spatial and temporal growth in the CABLH and the sudden rise in LHF during the convectively active case determined the convective activity associated off-shore trough along the west coast of India during ARMEX-I (2002). While the two cases of heavy rainfall were being studied, the heterogeneity in the convective atmosphere over the coast could be clearly observed.

The performance of the global spectral model NCMRWF GCM in simulating the CABL features using NLC-HP was tested. Spatial variation in CABL features, viz., LHF and CABLH, over the Arabian Sea off the west coast of India show the physical extent of convective activity during specific episodes of convection causing heavy rainfall. The diurnal variation is a little clearer from MM5 simulation. In a comparison of the MM5 simulations with the coarser grid NCMRWF GCM, the NCMRWF GCM underestimated the values of both LHF and CABLH. Results from MM5 indicate, therefore, that the best way forward in addressing the shortcomings of course grid-scale GCMs is to provide a parameterization of the diurnal effects associated with convection processes. This is necessary, since GCMs are not able to model explicitly the observed diurnal variability over convectively active regimes over the Indian seas.

Acknowledgements This study was financially supported by the Department of Science and Technology (DST). We are grateful for its valuable support. We also extend our sincere gratitude to the India Meteorological Department and the ARMEX experimental team for providing the data sets necessary to carry out the present study.

References

Asnani GC (1993) Tropical meteorology, 1st edn, vols I and II. Noble Printers, Pune, India, p 1202

Basu S, Iyengar GR, Mitra AK (2002) Impact of a non-local closure scheme in simulation of monsoon systems over India. Mon Weather Rev 130(1):161–170

Basu S, Raman S, Mohanty UC, Rajagopal EN (1999) Influence of the planetary boundary layer physics on medium-range prediction of monsoon over India. Pure Appl Geophys 155:33–55

Douglas SG, Kessler RC (1991) Analysis of mesoscale airflow patterns in the south central coast air basin during the SCCCAMP 1985 intensive measurement periods. J Appl Meteorol 30:607–631

Dudhia J, Gill D, Manning K, Wang W, Bruyere C (2002) PSU/NCAR mesoscale modeling system (MM5V3) tutorial class notes and user's guide (June). NCAR, Boulder, Colorado, USA

Fels SB, Schwarzkopf MD (1975) The simplified exchange approximation: a new method for radiative transfer calculations. J Atmos Sci 32:1475–1488

Grell GA, Dudhia J, Stauffer DR (1994) A description of the fifth generation Penn State/NCAR Mesoscale Model (MM5). National Center for Atmospheric Research Tech. Note NCAR/ TN-398, p 80

Hong S-Y, Pan H-L (1996) Nonlocal boundary layer vertical diffusion in a medium-range forecast model. Mon Weather Rev 124:2322–2339

Kanamitsu M (1989) Description of the NMC global data assimilation and forecast system. Weather Forecast 4:335–342

Krishnamurti TN, Cocke S, Pasch R, Low-Nam S (1983) Precipitation estimates from rain gauge and satellite observations: summer MONEX. Department of Meteorology, Florida State University, p 377

Lacis AA, Hansen JE (1974) A parameterization for the absorption of solar radiation in the Earth's atmosphere. J Atmos Sci 31:118–133

Lindzen RS (1981) Turbulence and stress owing to gravity wave and tidal breakdown. J Geophys Res 86:9707–9714

Meehl GA (1990) Seasonal cycle forcing of El Niño southern oscillation in a global, coupled ocean–atmosphere GCM. J Climate 3:72–89

Mohanty UC, et al (2002) Weather summary during ARMEX-2002, 2 vols, pp 1–157, A1–C40

Neelin JD (1990) A hybrid coupled general circulation model for El Niño studies. J Atmos Sci 47:674–693

Parish DF, Derber JC (1992) The NMC's spectral statistical interpolation analysis system. Mon Weather Rev 120:1747–1763

Rogers DP (1995) Air–sea interaction: connecting the ocean and atmosphere. In: US National Report to the IUGG, Quadrennial Report. American Geophysical Union

Sam NV (2005) Marine boundary layer and associated convective processes over Indian seas during Monsoons. PhD thesis, CAS, IIT Delhi

Sam NV, Mohanty UC, Kaur PS (2005) Conserved variable and observational analysis over the west-coast of India during ARMEX-2002. Mausam 56:201–212

Slingo J (1987) The development and verification of a cloud prediction scheme for the ECMWF model. Quart J Roy Meteor Soc 113:899–927

Tiedtke M (1983) The sensitivity of the time-mean large-scale flow to cumulus convection in the ECMWF model. Workshop on convection in large-scale models, ECMWF, 297–316

Ulrickson BL (1992) Effects of surface property variations on simulated daytime airflow over coastal southern California. Mon Weather Rev 120:2264–2279

Wilczak JM, Dabberdt WF, Kropfli RA (1991) Observations and numerical model simulations of the atmospheric boundary layer in the Santa Barbara coastal region. J Appl Meteorol 30:652–673